Available online at www.sciencedirect.com
ScienceDirect
Lithos 92 (2006) 524–536
LITHOS
www.elsevier.com/locate/lithos

Spinel–sapphirine–quartz bearing composite inclusion within garnet from an ultrahigh-temperature pelitic granulite: Implications for metamorphic history and *P–T* path

Toshiaki Tsunogae [a,b,*], M. Santosh [c]

[a] *Graduate School of Life and Environmental Sciences (Earth Evolution Sciences), University of Tsukuba, Ibaraki 305-8572, Japan*
[b] *Department of Geology, University of Johannesburg, P.O. Box 524, Auckland Park 2006, South Africa*
[c] *Faculty of Science, Kochi University, Akebono-cho 2-5-1, Kochi 780-8520, Japan*

Received 17 May 2005; accepted 30 March 2006
Available online 30 June 2006

Abstract

We report here a multiphase mineral inclusion composed of quartz, plagioclase, K-feldspar, sapphirine, spinel, orthopyroxene, and biotite, in porphyroblastic garnet within a pelitic granulite from Rajapalaiyam in the Madurai Granulite Block, southern India. In this unique textural association, hitherto unreported in previous studies, sapphirine shows four occurrences: (1) as anhedral mineral between spinel and quartz (Spr-1), (2) subhedral to euhedral needles mantled by quartz (Spr-2), (3) subhedral to anhedral mineral in orthopyroxene, and (4) isolated inclusion with quartz (Spr-4). Spr-1, Spr-2, and Spr-4 show direct grain contact with quartz, providing evidence for ultrahigh-temperature (UHT) metamorphism at temperatures exceeding 1000 °C. Associated orthopyroxene shows high Mg/(Fe+Mg) ratio (~ 0.75) and Al_2O_3 content (up to 9.6 wt.%), also suggesting $T>1050$ °C and $P>10$ kbar during peak metamorphism.

Coarse spinel (Spl-1) with irregular grain morphology and adjacent quartz grains are separated by thin films of Spr-1 and K-feldspar, suggesting that Spl-1 and quartz were in equilibrium before the stability of Spr-1+quartz. This texture implies that the *P–T* conditions of the rock shifted from the stability field of spinel+quartz to sapphirine+quartz. Petrogenetic grid considerations based on available data from the FMAS system favour exhumation along a counterclockwise *P–T* trajectory. The irregular shape of the inclusion and chemistry of the inclusion minerals are markedly different from the matrix phases suggesting the possibility that the inclusion minerals could have equilibrated from cordierite-bearing silicate-melt pockets during the garnet growth at extreme UHT conditions.

Keywords: Spinel+sapphirine+quartz; Granulite facies; Ultrahigh-temperature metamorphism; Counterclockwise *P–T* path; Madurai block; Southern India

1. Introduction

In recent years, our understanding of metamorphic processes in the continental deep crust underwent radical revision following the identification of a group of granulite–facies rocks that underwent extreme crustal metamorphism at $T=900$–1150 °C and $P=7$–13 kbar.

* Corresponding author. Graduate School of Life and Environmental Sciences (Earth Evolution Sciences), University of Tsukuba, Ibaraki 305-8572, Japan. Tel.: +81 29 853 5239; fax: +81 29 851 9764.
E-mail address: tsunogae@arsia.geo.tsukuba.ac.jp (T. Tsunogae).

0024-4937/$ - see front matter © 2006 Elsevier B.V. All rights reserved.
doi:10.1016/j.lithos.2006.03.060

Designated as ultrahigh-temperature (UHT) granulites (e.g. Harley, 1998, 2004), these rocks are characterized by typical mineral assemblages such as sapphirine+quartz (Dallwitz, 1968; Ellis et al., 1980; Grew, 1980), spinel+quartz (Friedman, 1953), orthopyroxene+sillimanite+quartz (Hensen and Green, 1973), osumilite+garnet (Ellis et al., 1980; Grew, 1982), inverted pigeonite (Grew, 1982; Sandiford and Powell, 1986; Harley, 1987; Tsunogae et al., 2002), and high-fluorine biotite and pargasite (Motoyoshi and Hensen, 2001; Tsunogae et al., 2003).

It has been commonly observed that the imprints of such UHT peak metamorphic conditions are obscured or overprinted by later high-temperature (e.g. 800 °C) retrograde metamorphism, especially in the presence of fluid. However, it is also known that the core of coarse-grained garnet is shielded against such overprints, and thus mineral assemblages preserved as inclusions in garnet cores from UHT rocks can provide robust information on the prograde history. Such inclusion minerals have been studied by several authors for reconstructing the prograde *P–T* path and/or estimating the peak metamorphic conditions (e.g. Lal, 2003). Of particular relevance in this context are those UHT metamorphic terranes such as those from the Pan-African granulite terranes in South India, Sri Lanka, and Antarctica, which underwent multiple thermal events of high-temperature (~900 °C) overprinting the earlier events such that the matrix mineral assemblages were frequently reset and the peak assemblages are preserved only as inclusion minerals within porphyroblastic garnet (Sajeev and Osanai, 2004; Tateishi et al., 2004; Das et al., 2006). Hence, detailed investigations on mineral inclusions in garnet are of potential significance in our understanding of the *P–T* history of high-grade metamorphic rocks.

In this study, we report multiphase mineral inclusions enclosed within porphyroblastic garnet in a pelitic granulite from Rajapalaiyam in the southern part of the Madurai Block, southern India. The assemblages and textures reported in this study from the garnet-hosted composite mineral inclusions are unique, and have not been documented from any UHT rocks so far. The Rajapalaiyam area is a key location in southern India for UHT metamorphism, from where we recently reported equilibrium sapphirine+quartz assemblage in quartzo-feldspathic and pelitic granulites for the first time from southern India (Tateishi et al., 2004), providing robust evidence for $T>1000$ °C UHT metamorphism (e.g. Bertrand et al., 1991; Kelsey et al., 2004). Our further detailed studies on this area led to the finding of unique multiphase inclusions in

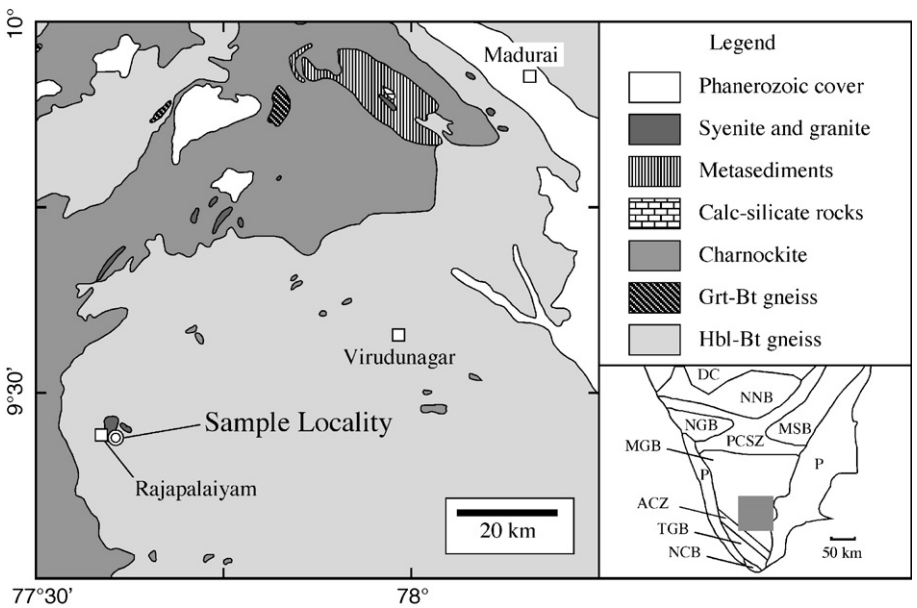

Fig. 1. Geological map of the Madurai Block (based on 1:500,000 map of Tamil Nadu, GSI, 1995) with the sample locality of pelitic granulite from Rajapalaiyam discussed in this paper. The Madurai Block is composed mainly of charnockite and hornblende–biotite gneiss. Boundary between the two lithologies is gradual, but local replacement of charnockite by hornblende–biotite gneiss is commonly observed. DC: Dharwar Craton, MGB: Madurai Block, MSB: Madras Block, NNB: Northern Block, NGB: Nilgiri Block, TGB: Trivandrum Block, NCB: Nagarcoil Block, ACZ: Achankovil Shear Zones, PCSZ: Palghat-Cauvery Shear Zone, P: Phanerozoic cover.

garnets, which we document in this paper. Based on detailed petrological studies of these assemblages, we attempt to construct the *P–T* history of the rock. Our results are important in understanding the metamorphic history of the Madurai Block as well as in evaluating the tectonics of continent–continent collision during Pan-African orogeny in southern India associated with the final assembly of the Gondwana supercontinent (e.g. Santosh et al., 2003).

2. General geology

Rajapalaiyam is located about 80 km southwest of Madurai City (Fig. 1) in the Tamil Nadu state of southern India. The lithologic units in this region comprise massive charnockite and associated lenses of pelitic and calc–silicate rocks. Late intrusions of pink alkali–feldspar granites are also recognized from the area. Sapphirine-bearing quartzo-feldspathic and pelitic gra-

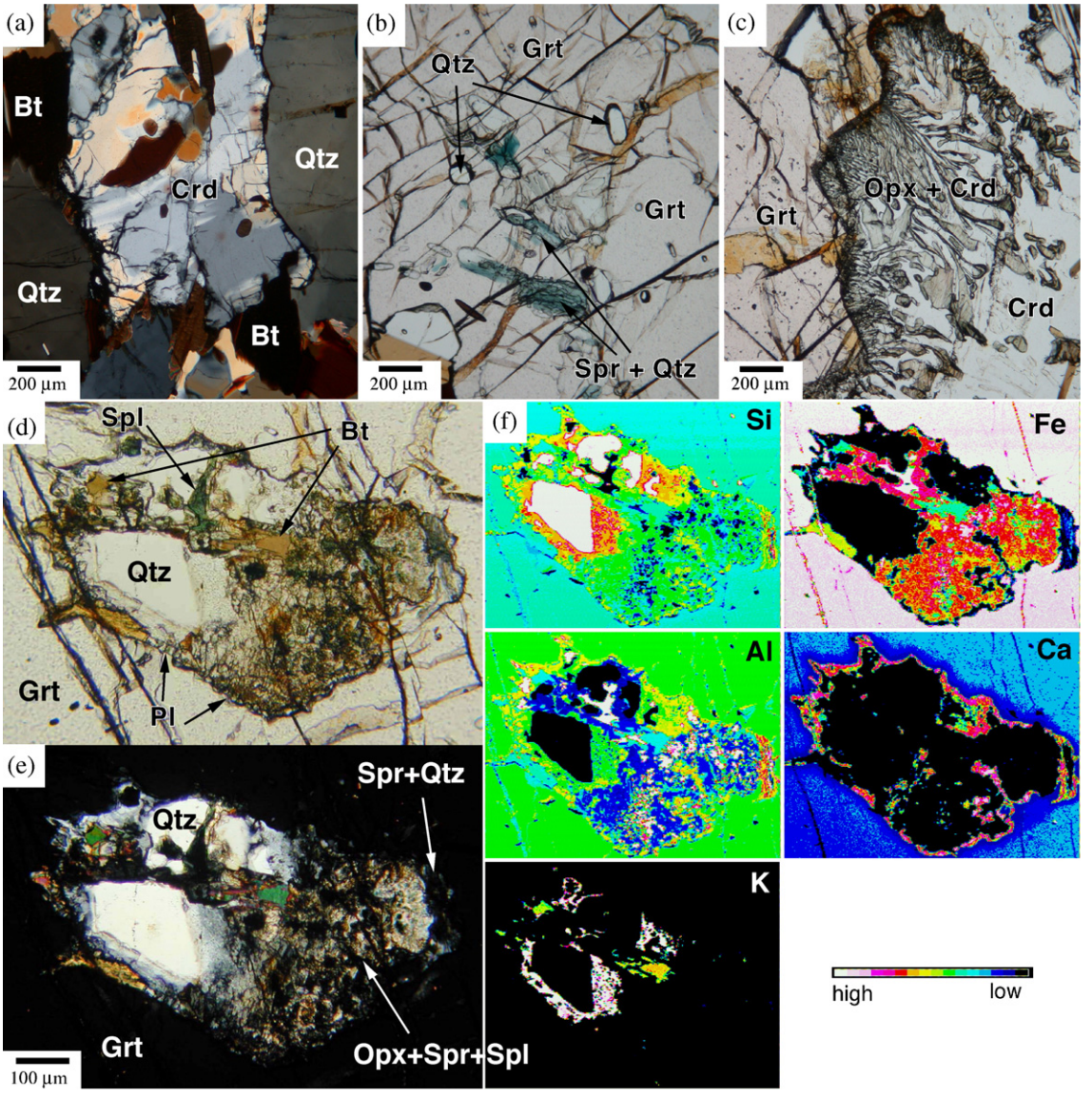

Fig. 2. Photomicrographs of various textures in sample MD6-2E2. (a) Subhedral cordierite in quartzo-feldspathic layer. Crossed polars. (b) Poikiloblastic garnet with inclusions of sapphirine+quartz. Polarized light. (c) Cordierite+orthopyroxene corona around garnet. (d) Multiphase inclusion in garnet. Polarized light. (e) Same as above. Crossed polars. (f) Compositional mapping showing distribution of elements (Si, Al, K, Fe, and Ca) within the multiphase inclusions. Note that Ca content of garnet decreases adjacent to the inclusion.

nulites occur as layered gneisses of about 20 m in thickness within charnockitic lithologies in association with pink granite. The granulite shows various mineral assemblages such as quartz+mesoperthite+garnet, orthopyroxene+biotite+garnet, orthopyroxene+sapphirine+garnet and cordierite+orthopyroxene+quartz (Tateishi et al., 2004). Sriramguru et al. (2002) first reported sapphirine in this locality from within pelitic enclaves (garnet+orthopyroxene+cordierite+spinel+plagioclase+perthite) in the alkali–feldspar granite, and determined peak temperatures of 860 °C from garnet–orthopyroxene geothermometer and 950 °C from feldspar thermometer on mesoperthite. Tateishi et al. (2004) conducted a more detailed study in this area and discovered sapphirine+quartz assemblage and high Al content in orthopyroxene (up to 9.7 wt.% Al_2O_3). They estimated the peak metamorphic P–T conditions of the area as $T>1050$ °C and $P=9$–10 kbar. From garnet–cordierite–sillimanite association around sapphirine+quartz and various decompression textures such as orthopyroxene+cordierite+sapphirine, spinel+cordierite, and sapphirine+orthopyroxene around garnet porphyroblast, Tateishi et al. (2004) inferred early isobaric cooling from the stability field of sapphirine+quartz to ca. 1030–1040 °C followed by near isothermal decompression down to 950 °C and 7–8 kbar. In contrast, no evidence of UHT metamorphism has been found from adjacent lithologies (e.g. charnockite) probably because of

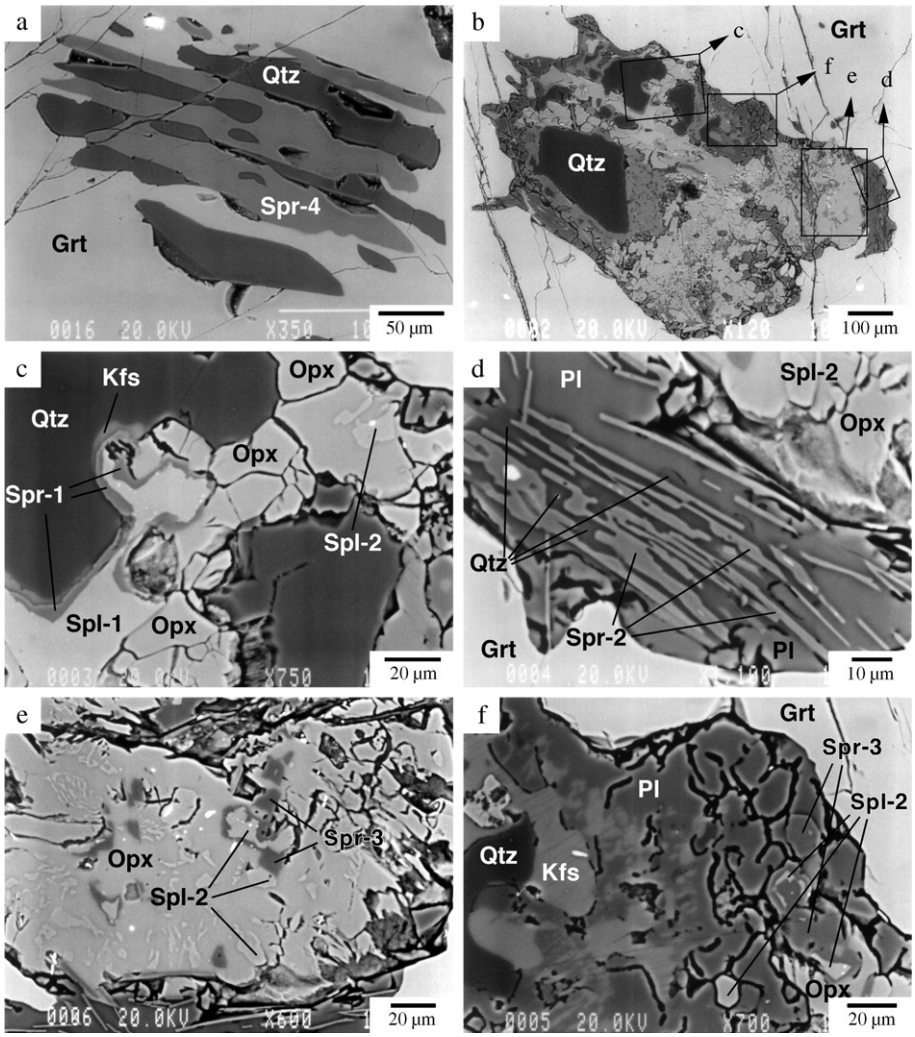

Fig. 3. Back-scattered electron images showing detailed textures of mineral inclusions in garnet in sample MD6-2E2. (a) Equilibrium Spr-4+quartz assemblage enclosed in garnet. (b) An overview of the multiphase mineral inclusion in garnet. (c) Spr-1+Spl-1 associated with quartz. (d) Subhedral to euhedral elongated Spr-2 included in quartz. (e) Association of Spr-3 and Spl-2 in orthopyroxene aggregates. (f) Intergrowth of Spl-2 with Spr-3 and orthopyroxene. Aggregates of plagioclase occur along the margin of the composite inclusion.

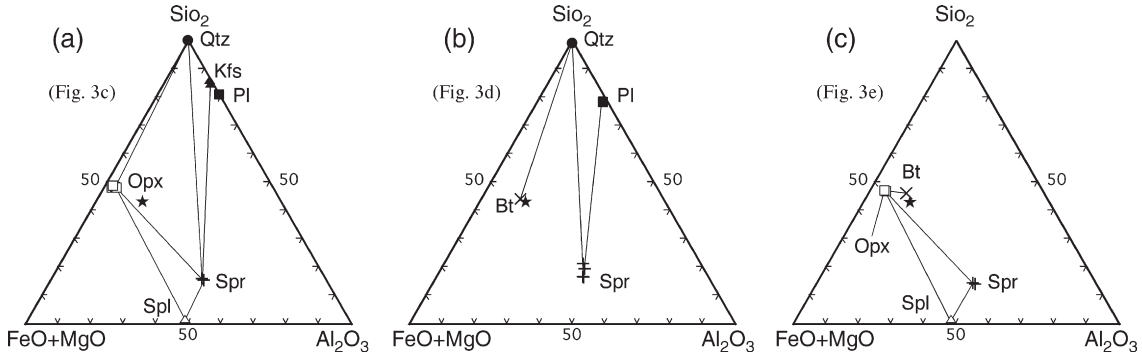

Fig. 4. SiO_2–(FeO+MgO)–Al_2O_3 diagrams showing mineral assemblages and chemistry for the examined multiphase inclusion. Stars denote averaged composition of host garnet. (a) Sapphirine–spinel–quartz–orthopyroxene assemblage in Fig. 3c. (b) Sapphirine+quartz assemblage in Fig. 3d. (c) Sapphirine–spinel–orthopyroxene assemblage in Fig. 3e.

their high SiO_2-rich bulk chemistry and lack of appropriate UHT mineral assemblages.

3. Petrography

Below we describe petrography of the pelitic granulite (sample MD6-2E2) from Rajapalaiyam examined in detail in this study. The sample was collected from the same locality where Tateishi et al. (2004) reported sapphirine+quartz and high-Al orthopyroxene (up to 9.7 wt.%). The textural features are shown in Figs. 2 and 3. Mineral abbreviations are after Kretz (1983). Representative mineral assemblages are shown in triangular diagrams (Fig. 4).

The pelitic granulite in this locality is composed of quartz–feldspar-rich leucocratic layer and garnet–cordierite–biotite-rich melanocratic layer. Foliation of the rock is defined by alternation of the layers. Mineral lineation is not obvious. The leucocratic layer is composed of quartz (~8 mm), mesoperthite (~1.4 mm), and cordierite (~1.2 mm) with minor biotite (~2 mm) and sillimanite (0.1–0.8 mm) (Fig. 2a). Such quartzo-feldspathic layers or lenses are dominant in pelitic granulites of the examined outcrop as discussed by Tateishi et al. (2004). Relatively coarse-grained nature of the minerals as well as their randomly oriented characters may suggest a partial melting origin of the layer. The dominant mineral assemblage of the melanocratic layer is garnet+cordierite+orthopyroxene+quartz+sillimanite+biotite. Accessory minerals are rutile, ilmenite, and sapphirine, but sapphirine is present only in garnet. Garnet in the sample forms very coarse-grained porphyroblastic aggregates (up to 3 cm) and contains numerous monophase and multiphase mineral inclusions (Table 1). The individual aggregate is composed of several domains, with size varying from 0.3 to 15 mm in length. The garnets contain inclusions of quartz, sapphirine, sillimanite, ilmenite, plagioclase, K-feldspar, rutile,

Table 1
Mineral assemblages of multiphase inclusions enclosed in garnet in sample MD6-2E2

Inclusion no.	size (μm)	Qtz	Pl	Kfs	Spr	Spl	Opx	Bt	Grt	Sil	Crd	Chl	Zrn	Ap	Textures
1	930×480	+++	++	+	+	+	++	++							1, 2, 3, 4
2	470×140	++			++										1
3	250×130	+++	++	++				+							4
4	450×280	+++						++				+*			
5	510×230	+++			++			++				+*			1
6	250×230	+++						+							
7	310×150	+++			++			++							1
matrix1**	–	++	+	+			++	++	+++	+	++		+	+	5
matrix2**	–	+++	++	++			+	+	+	+	++		+	+	

Inclusion 1 corresponds to the multiphase inclusion discussed in the text.
+++: abundant, ++: moderate, +: rare, *: retrograde mineral.
1: sapphirine+quartz, 2: spinel+quartz, 3: sapphirine+orthopyroxene+spinel intergrowth, 4: mesoperthite, 5: cordierite+orthopyroxene corona around garnet.
**: matrix1: matrix mineral assemblage (melanocratic), matrix2: matrix mineral assemblage (leucocratic).

zircon, and monazite (Fig. 2b) as well as a multiple mineral inclusion discussed later. The sapphirine inclusions (Spr-4) occasionally coexist with quartz (Fig. 3a), suggesting that the garnet crystallized within or close to the stability field of sapphirine+quartz. The garnet also shows a retrogade decompression texture characterized by coronas of cordierite+orthopyroxene (Fig. 2c). The texture suggests the following common decompression reaction:

$$\mathrm{Grt} + \mathrm{Qtz} \rightarrow \mathrm{Opx} + \mathrm{Crd} \quad (1)$$

As discussed in a later section of this paper, the pyrope content of the garnet decreases slightly from core toward rim due to the higher Mg content of the products, orthopyroxene and cordierite. Since the thickness of the reaction corona around garnet is less than 1 mm in the studied sample (Fig. 2c), we conclude that retrograde metamorphism did not significantly affect the interior of the garnet.

The unique multiphase mineral inclusion that we report here is 0.5×0.9 mm in size and ovoidal in shape, occurring within the core portion of a coarse-grained (12 mm in diameter) porphyroblastic garnet (Figs. 2d, e and 3b). The distance from the inclusion to the grain margin of the host garnet is 3 mm and no effect of any retrograde imprint is found, although rim of the garnet grain is partly mantled by corona of orthopyroxene+cordierite due to the progress of reaction (1). The multiphase inclusion is composed of fine-grained aggregates of quartz, plagioclase, K-feldspar, sapphirine, spinel, orthopyroxene, and biotite. Distribution of the minerals is heterogeneous except in the case of plagioclase, which mostly occurs along the margin of the inclusion (e.g. Fig. 2f). As shown in the back-scattered image of the composite inclusion (Fig. 3b), quartz is the most dominant mineral and constitutes about 25% of the inclusion aggregate. It shows rounded shape and is in contact with various minerals such as K-feldspar, plagioclase, orthopyroxene, and sapphirine. As shown in Fig. 3c, sapphirine and quartz show a direct grain contact with no reaction texture visible between the two, although a very thin film of K-feldspar occasionally occurs between the two minerals (Fig. 4a). Sapphirine shows three modes of occurrences in the multiple inclusion; as anhedral mineral between spinel and quartz (Spr-1; Fig. 3c), needle-shaped subhedral to euhedral phase in quartz (Spr-2; Fig. 3d), and subhedral to anhedral mineral partly surrounding spinel and included within orthopyroxene (Spr-3; Fig. 3e). Spr-1 occurs as a thin (<50 μm) film between spinel and quartz. Spr-2 needle is up to 100 μm in length and is apparently oriented. Most of them are included in single quartz grain, although some are also found in plagioclase mantling the quartz (Fig. 4b). Spr-3 occurs as anhedral mineral of up to 20 μm scattered in orthopyroxene aggregate and commonly surrounding spinel. As discussed later, the three varieties of sapphirine show marked compositional differences suggesting their distinct paragenesis. Spr-4, which is also discussed later, occurs as isolated inclusions with quartz in the same garnet grain. Spinel is either associated with sapphirine (Spl-1; Fig. 3c) or occurs as inclusions in orthopyroxene (Spl-2; Figs. 3e, f and 4c). Although spinel does not show direct grain contact with quartz, the largest Spl-1 grain (~100 μm) clearly surrounds some quartz grains (Fig. 3b, c). This texture suggests that spinel and quartz were once in equilibrium, and that later sapphirine formed between the two minerals. The following FMAS continuous reaction can be deduced to explain the formation of sapphirine from spinel and quartz:

$$\mathrm{Spl} + \mathrm{Sil} + \mathrm{Qtz} \rightarrow \mathrm{Spr}_{[7:9:3]} \quad (2)$$

As discussed in the next section sapphirine has two end members on the basis of (Mg, Fe)O:Al_2O_3:SiO_2 ratio; 7:9:3 and 2:2:1. As Spr-1 chemistry is close to the 7:9:3 end member or even more aluminous, sillimanite is required as a reactant phase to form sapphirine$_{[7:9:3]}$, although sapphirine$_{[2:2:1]}$ can be formed directly from spinel+quartz. Although sillimanite could not be observed in the inclusion, it is a common phase in the matrix and also occurs as inclusions within the garnet porphyroblast. We infer that reaction (2) took place within the stability field of sapphirine+quartz. Spl-2 (5–25 μm) shows irregular shape and occurs as in intergrowth with orthopyroxene and sapphirine (Fig. 3e, f).

Fine blades of orthopyroxene (20–50 μm crystals) occur as aggregates of up to 150 μm size. Some of the grains are intergrown with spinel, although homogeneous grains in the absence of sapphirine and spinel are also present. Plagioclase (10–100 μm) is mainly scattered along the margin of the multiphase inclusion (Figs. 2f and 3f) or mantle the quartz (Fig. 3d). Rarely, it occurs as lamella in K-feldspar as perthite. The perthite is relatively coarse-grained (~130 μm) and occurs mainly around quartz, probably suggesting the possible presence of a quartzo-feldspathic melt. Biotite is relatively coarse-grained (~130 μm) and occurs together with quartz and perthite.

4. Mineral chemistry

Chemical analyses of minerals were performed by electron microprobe analyzer (JEOL JXA8621) at the Chemical Analysis Division of the Research Facility

Table 2
Representative electron microprobe analyses of minerals in sample MD6-2E2 discussed in this study

Mineral name	Spr-1*	Spr-1*	Spr-2*	Spr-2*	Spr-3*	Spr-3*	Spr-4	Spr-4	Spl-1*	Spl-1*	Spl-2*	Spl-2*	Opx*	Opx*
O**	20 with Spl-1	20 with Spl-1	20 +Qtz	20 +Qtz	20 with Spl-2	20 with Spl-2	20 +Qtz	20 +Qtz	4 with Spr-1	4 with Spr-1	4 with Spr-3	4 with Spr-3	6 with Spl-2	6 with Pl
SiO_2	11.64	12.26	13.83	13.62	11.10	11.14	13.55	13.34	0.02	0.03	0.03	0.08	50.02	50.59
Al_2O_3	65.01	63.14	61.33	61.64	66.27	64.33	59.30	59.10	63.66	63.81	64.52	63.58	9.64	9.24
TiO_2	0.01	0.05	0.00	0.01	0.04	0.00	0.06	0.06	0.09	0.00	0.01	0.01	0.07	0.08
Cr_2O_3	0.04	0.01	0.08	0.02	0.05	0.09	0.08	0.11	0.06	0.06	0.09	0.12	0.01	0.00
Fe_2O_3									1.98	2.23	2.48	1.92		
FeO	6.69	6.58	6.50	6.24	5.83	6.27	9.38	8.71	18.94	18.88	16.96	17.29	15.05	14.57
MnO	0.00	0.00	0.00	0.00	0.02	0.03	0.00	0.00	0.00	0.00	0.08	0.00	0.04	0.04
MgO	16.51	16.73	16.53	16.64	16.39	16.44	16.73	16.76	14.95	15.04	16.34	15.78	26.14	26.88
ZnO	0.10	0.11	0.08	0.09	0.12	0.11	0.06	0.08	0.30	0.37	0.51	0.46	0.07	0.13
CaO	0.00	0.01	0.03	0.00	0.03	0.00	0.00	0.02	0.00	0.00	0.00	0.01	0.00	0.01
Na_2O	0.04	0.06	0.02	0.00	0.01	0.00	0.01	0.00	0.02	0.01	0.01	0.02	0.02	0.01
K_2O	0.04	0.03	0.00	0.00	0.00	0.00	0.01	0.02	0.01	0.00	0.01	0.00	0.01	0.00
Total	100.08	98.98	98.39	98.26	99.85	98.42	99.17	98.21	100.02	100.43	101.03	99.25	101.07	101.54
Si	1.381	1.470	1.663	1.638	1.315	1.343	1.643	1.630	0.001	0.001	0.001	0.002	1.778	1.786
Al	9.089	8.921	8.690	8.735	9.247	9.136	8.474	8.508	1.957	1.954	1.950	1.956	0.404	0.384
Ti	0.001	0.004	0.000	0.001	0.003	0.000	0.006	0.006	0.002	0.000	0.000	0.000	0.002	0.002
Cr	0.004	0.001	0.008	0.002	0.005	0.008	0.007	0.011	0.001	0.001	0.002	0.002	0.000	0.000
Fe^{3+}	0.145	0.138	0.000	0.000	0.119	0.170	0.233	0.221	0.039	0.044	0.048	0.038		
Fe^{2+}	0.518	0.522	0.653	0.627	0.459	0.462	0.718	0.668	0.413	0.410	0.364	0.377	0.447	0.430
Mn	0.000	0.000	0.000	0.000	0.002	0.003	0.000	0.000	0.000	0.000	0.002	0.000	0.001	0.001
Mg	2.918	2.988	2.961	2.981	2.892	2.952	3.022	3.050	0.581	0.582	0.624	0.614	1.384	1.413
Zn	0.009	0.010	0.007	0.008	0.010	0.010	0.005	0.007	0.006	0.007	0.010	0.009	0.002	0.003
Ca	0.000	0.002	0.003	0.001	0.003	0.000	0.000	0.003	0.000	0.000	0.000	0.000	0.000	0.000
Na	0.010	0.015	0.005	0.000	0.003	0.000	0.002	0.000	0.001	0.001	0.001	0.001	0.002	0.001
K	0.006	0.005	0.000	0.000	0.000	0.000	0.002	0.004	0.000	0.000	0.000	0.000	0.000	0.000
Total	14.080	14.075	13.990	13.993	14.057	14.085	14.112	14.107	3.000	3.000	3.000	3.000	4.019	4.020
Mg/(Fe+Mg)	0.85	0.85	0.82	0.83	0.86	0.86	0.81	0.82	0.58	0.59	0.63	0.62	0.76	0.77
Ca/(Ca+Na+K)														

*: minerals in the multiple inclusion.
**: number of oxygens.

Center for Science and Technology, University of Tsukuba for all minerals. The analyses were performed under conditions of 20 kV accelerating voltage and 10 nA sample current, and the data were regressed using an oxide-ZAF correction program supplied by JEOL. Representative compositions of minerals in the analyzed sample are given in Table 2. Fe^{3+} of sapphirine given in the table has been calculated after Higgins et al. (1979). Fe^{3+} of spinel was calculated based on stoichiometry. The X_{Mg} [=Mg/(Fe^{2+}Mg)] ratios for the relevant phases have the following order: sapphirine (0.80–0.87)> biotite (0.82–0.83)>orthopyroxene (0.76–0.77)>spinel (0.58–0.63)>garnet (0.54–0.56). Mineral assemblages and chemistry are shown in triangular diagrams (Fig. 4).

4.1. Sapphirine

Sapphirine in the examined sample is texturally divided into four types; Spr-1 to Spr-3 within the multiphase inclusion and Spr-4 which occurs as an isolated inclusion with quartz. Their compositional variations are shown in Fig. 5. Spr-1 and Spr-3 exhibit highly magnesian compositions (X_{Mg}=0.84–0.87) close to the 7:9:3 end member (Table 2, Fig. 5). Spr-2 and Spr-4, which are mostly associated with quartz, show lower X_{Mg} (0.80–0.83) and higher Si content (1.6–1.7 pfu) than the other two types. The results are consistent with the observation of Ouzegane and Boumaza (1996) who reported that sapphirine in association with quartz contains higher Si than that occurring in the absence of quartz. Other components total less than 0.2 wt.%. All the data show MgSi=2Al tschermak substitution between the 7:9:3 and 2:2:1 end members. Spr-1, 3, and 4 plot slightly below the substitution line due to the presence of Fe^{3+}. The calculated $Fe^{3+}/(Fe^{2+}Fe^{3+})$ ratio using the method of Higgins et al. (1979) is 0.08–0.26 for the three types. On the other hand, $Fe^{3+}/(Fe^{2+}Fe^{3+})$ of Spr-2 is significantly low (<0.07).

4.2. Spinel

Spinel occurs only in the multiphase inclusion in the examined sample. It is dominantly a solid solution of

Opx* 6 with PI	Opx 6 matrix	Opx 6 symplectite	Grt 12 core	Grt 12 rim	Kfs* 8	Pl* 8 in Kfs	Pl* 8	Pl 8 matrix	Bt* 22	Bt 22 matrix	Bt 22 matrix	Crd 18 symplectite	Crd 18 matrix
50.69	47.87	49.41	40.16	39.95	65.15	63.35	59.97	61.66	37.94	37.64	36.96	50.45	49.31
8.92	8.65	7.83	22.74	22.92	18.66	23.70	25.12	23.77	16.39	15.81	15.04	33.72	33.35
0.09	0.14	0.12	0.01	0.00	0.03	0.02	0.00	0.00	4.38	4.18	5.93	0.01	0.02
0.06	0.10	0.22	0.01	0.07	0.00	0.00	0.00	0.00	0.02	0.11	0.20	0.02	0.02
14.43	19.68	20.78	24.15	24.07	0.09	0.08	0.23	0.25	7.20	10.72	11.98	3.43	3.74
0.00	0.03	0.01	0.09	0.12	0.00	0.00	0.00	0.00	0.02	0.04	0.03	0.00	0.00
26.71	22.63	22.63	13.08	12.80	0.00	0.03	0.01	0.00	19.56	16.99	15.23	11.61	11.27
0.16	0.00	0.00	0.00	0.00	0.07	0.07	0.14	0.11	0.13	0.09	0.12	0.00	0.01
0.00	0.04	0.04	0.69	0.70	0.01	4.33	6.83	4.81	0.00	0.00	0.00	0.02	0.00
0.02	0.00	0.04	0.02	0.00	1.29	8.96	8.24	8.95	0.15	0.22	0.29	0.02	0.05
0.00	0.02	0.00	0.00	0.00	14.81	0.15	0.15	0.39	9.84	9.57	9.48	0.00	0.00
101.07	99.15	101.06	100.94	100.62	100.11	100.69	100.69	99.95	95.62	95.37	95.25	99.28	97.76
1.796	1.777	1.804	2.992	2.987	2.993	2.782	2.665	2.745	5.451	5.508	5.465	5.025	4.998
0.372	0.378	0.337	1.997	2.019	1.010	1.226	1.315	1.247	2.774	2.727	2.621	3.957	3.983
0.002	0.004	0.003	0.001	0.000	0.001	0.001	0.000	0.000	0.473	0.460	0.659	0.000	0.002
0.002	0.003	0.006	0.001	0.004	0.000	0.000	0.000	0.000	0.002	0.013	0.023	0.002	0.002
0.427	0.611	0.634	1.504	1.504	0.003	0.003	0.009	0.009	0.865	1.312	1.480	0.286	0.317
0.000	0.001	0.000	0.006	0.007	0.000	0.000	0.000	0.000	0.003	0.004	0.004	0.000	0.000
1.410	1.252	1.231	1.452	1.425	0.000	0.002	0.000	0.000	4.185	3.704	3.355	1.722	1.701
0.004	0.000	0.000	0.000	0.000	0.002	0.002	0.005	0.004	0.014	0.010	0.014	0.000	0.000
0.000	0.002	0.002	0.055	0.056	0.001	0.203	0.325	0.229	0.000	0.000	0.000	0.003	0.000
0.001	0.000	0.003	0.003	0.000	0.115	0.762	0.709	0.772	0.041	0.063	0.083	0.003	0.009
0.000	0.001	0.000	0.000	0.000	0.867	0.008	0.009	0.022	1.803	1.786	1.787	0.000	0.000
4.015	4.029	4.020	8.010	8.002	4.992	4.990	5.036	5.029	15.610	15.586	15.490	10.997	11.012
0.77	0.67	0.66	0.49	0.49					0.83	0.74	0.69	0.86	0.84
						0.21	0.31	0.22					

hercynite and Mg-spinel (X_{Mg}=0.58–0.63). The calculated $Fe^{3+}/(Fe^{2+}Fe^{3+})$ ratio (<0.12) is lower than that of Spr-1, 3, and 4. Although spinel occurs both with sapphirine (Spl-1; Fig. 3c) and as inclusions in orthopyroxene (Spl-2; Fig. 3e), there is no significant compositional difference between the two types. Only slight enrichment in Cr_2O_3 and ZnO is observed in Spl-2 (0.09–0.14 wt.% and 0.38–0.51 wt.%, respectively) as compared to Spl-1 (0.06–0.08 wt.% and 0.29–0.37 wt. %, respectively).

4.3. Orthopyroxene

Orthopyroxene within the composite inclusion is Mg-rich in composition with X_{Mg}=0.76–0.77. The X_{Mg} ratio is significantly higher than the matrix coarse-grained (up to 1 mm) orthopyroxene (X_{Mg}=0.66–0.69) and symplectitic fine-grained orthopyroxene (X_{Mg}=0.65–0.67) associated with cordierite (Fig. 6). The Al_2O_3 content of the orthopyroxene in the multiphase inclusion shows a wide range of 6.7 to 9.6 wt.% (Al [pfu]=0.28–0.40) depending on coexisting minerals. That of matrix and symplectitic phases is also high (up to 8.6 wt.% and 7.8 wt.%, respectively).

4.4. Garnet

Garnet is the host mineral of the multiphase inclusion and is essentially a solid solution of pyrope and almandine (X_{Mg}=0.46–0.50) with low contents of spessartine (<1 mol%) and grossular (<3 mol%). The garnet shows a slight rimward decrease of pyrope content; from $Alm_{49–50}$ $Pyr_{48–49}$ $Grs_{1–2}$ $Sps_{0–1}$ at the core to $Alm_{50–51}$ $Pyr_{47–48}$ $Grs_{1–2}$ $Sps_{0–1}$ at the rim in contact with quartz. The garnet rim in contact with cordierite+orthopyroxene symplectite shows the highest almandine content of $Alm_{52–53}$ $Pyr_{44–45}$ $Grs_{3–4}$ $Sps_{0–1}$, suggesting the progress of reaction (1). Fine-grained garnet inclusion in Spr-4 shows the highest pyrope content of $Alm_{45–46}$ $Pyr_{52–53}$ $Grs_{2–3}$ $Sps_{0–1}$. Fig. 2f demonstrates that grossular content of garnet slightly decreases near the contact with the multiphase inclusion. This is probably due to the presence of plagioclase along the contact. It is possible that some amount of Ca was

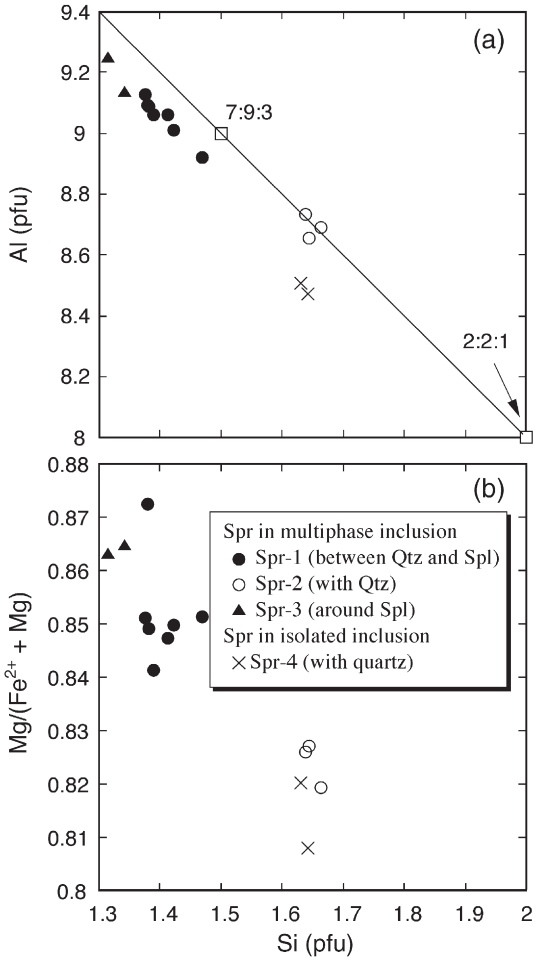

Fig. 5. Compositional diagrams showing sapphirine chemistry. 7:9:3 and 2:2:1 in the figure imply end member compositions of $Mg_{1.75}Al_{4.5}Si_{0.75}O_{10}$ and $Mg_2Al_4SiO_{10}$, respectively.

incorporated into the plagioclase at the time of high-grade metamorphism.

4.5. Biotite

Biotite associated with plagioclase shows high X_{Mg} ratio (0.82–0.83) compared to the matrix phase (0.80). The TiO_2 contents of both categories are high, in the range of 3.8–4.4 wt.%. They also show similar fluorine and chlorine contents of 0.6–1.3 wt.% and 0.01–0.09 wt.%, respectively.

4.6. Feldspar

Plagioclase in the inclusion is rich in albite, and shows two compositional ranges depending on the mode of occurrence. Plagioclase lamella in K-feldspar has a higher albite content as $An_{20–21}$ $Ab_{78–79}$ $Or_{0–1}$. On the other hand, coarse-grained plagioclase along the inclusion–garnet boundary has slightly higher anorthite content as $An_{28–32}$ $Ab_{68–71}$ $Or_{0–1}$. The latter composition is consistent with an isolated plagioclase inclusion in the same garnet grain. K-feldspar composition is close to the orthoclase end member as $An_{0–1}$ $Ab_{11–14}$ $Or_{86–89}$.

5. Metamorphic *P–T* conditions

Several geothermobarometers are applicable for the multiple inclusions within garnet from Rajapalaiyam due to the presence of a number of ferromagnesian minerals. Although some of the computations based on conventional Fe–Mg exchange reactions are not suitable for UHT rocks to infer the peak *P–T* conditions due to the effect of retrograde thermal events, such procedures are useful to infer the retrograde *P–T* conditions.

5.1. Sapphirine–spinel geothermometers

As shown in Fig. 3e, Spr-3 and Spl-2 coexist with no reaction texture seen between them, although both are included within orthopyroxene. We therefore regard the two minerals to be in equilibrium, and apply the sapphirine–spinel geothermometers to the mineral pairs. Owen and Greenough (1991) proposed a geothermometer based on the Fe–Mg exchange reaction between sapphirine and spinel. The method is based on empirical determination of entropy and enthalpy of the reaction. Results using this computation yielded a temperature range of 860–890 °C. If we consider the effect of Fe^{3+} in sapphirine and spinel, the above temperature estimate would be enhanced by about 40 °C as 900–920 °C, an estimate that is still significantly lower than the stability temperature of sapphirine and

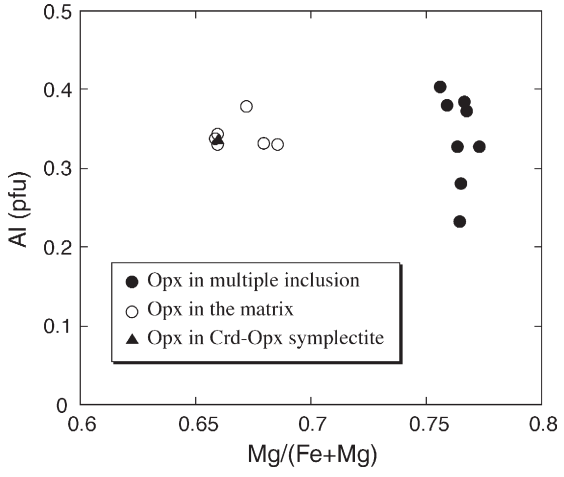

Fig. 6. Compositional diagram showing orthopyroxene chemistry.

quartz. Das et al. (2003) formulated a new sapphirine–spinel geothermometer using their experimental data at 9–12 kbar and 850–1100 °C. Application of this method yielded almost consistent results in the range of 820–850 °C. In contrast, application of the geothermometers to Spr-1 and Spl-1 pairs gave slightly lower temperatures of 820–830 °C.

5.2. Garnet–orthopyroxene geothermometer

The garnet–orthopyroxene thermometer was applied to the orthopyroxene aggregate and the host garnet. The estimated temperature range for garnet–orthopyroxene pairs is 800–850 °C at 8 kbar using the method of Lee and Ganguly (1988), which is based on experimental calibration of Fe–Mg fractionation between garnet and orthopyroxene in FMAS system at 20–45 kbar and 975–1400 °C. The range from Aranovich and Berman's (1997) method (780–870 °C at 8 kbar), a formulation based on Al solubility in orthopyroxene, is almost consistent. Calculated temperature ranges from the method of Harley and Green (1982), which is based on experimental data of the mineral pairs at 5–20 kbar and 800–1200 °C, are 820–950 °C at 8 kbar.

5.3. Sapphirine–orthopyroxene geothermometer

Kawasaki and Sato (2002) experimentally obtained a geothermometer using natural sapphirine–orthopyroxene assemblage for the application to UHT metamorphic rocks. The method was applied to Spr-3 and host orthopyroxene, which are texturally in equilibrium (Fig. 3e). The result yielded a temperature range of 820–900 °C, which is almost conformable with the results from sapphirine–spinel and garnet–orthopyroxene geothermometers.

5.4. Garnet–orthopyroxene–plagioclase–quartz geobarometer

The geobarometer was applied to host garnet, plagioclase along the inclusion margin, and orthopyroxene adjacent to the plagioclase grain. According to the calibration of Perkins and Newton (1981), we obtained a pressure range of 7.7–8.3 kbar at 1000 °C (see below for peak temperature estimate). The refined method of Perkins and Chipera (1985) also gave a similar pressure range of 7.9–8.4 kbar at the same temperature.

5.5. Al solubility in orthopyroxene

The Al content and X_{Mg} of orthopyroxene coexisting with garnet, sillimanite (or cordierite), and quartz are potential indicators of *P–T* conditions. Based on the isotherms and isobars of the theoretical study by Hensen and Harley (1990), the orthopyroxene in the multiphase inclusion equilibrated at a *P–T* range of >1000 °C and >10 kbar. Harley (1998) revised the isopleths of Hensen and Harley (1990) using new experimental results (e.g. Carrington and Harley, 1995). The estimated results using Harley's (1998) isopleths are about 50 °C lower than those given by Hensen and Harley's (1990) method, although they are still around 950–970 °C. Application of Al_2O_3 isopleth of Harley (2004) yielded similar temperature ranges of T=900–1000 °C at 10 kbar, which also suggests UHT conditions during peak metamorphism in this area.

6. Discussion

The unique textural association of quartz, plagioclase, K-feldspar, sapphirine, spinel, orthopyroxene, and biotite, within porphyroblastic garnet in pelitic granulites from Rajapalaiyam area in the Madurai Granulite Block provides important clues on UHT metamorphism in southern India. Mineral chemistry data suggest that compositions of orthopyroxene and biotite in the multiphase inclusion are significantly Mg-rich than those in the matrix phases. Fig. 5 shows that sapphirines in the multiphase inclusion (Spr-1, 2, and 3) are slightly different in Si and Al contents than Spr-4 (+quartz) which is included in a different garnet grain (Figs. 2b and 3a). Spinel is absent in the matrix, yet X_{Mg} of Spl-1 and Spl-2 (0.58–0.63) is higher than that in adjacent lithologies (0.47–0.54; Tateishi et al., 2004). The mineral chemistry results therefore suggest that ferromagnesian minerals in the multiphase inclusion formed from a precursor that is distinct as compared to the one from which the matrix minerals were derived. The irregular shape of the inclusion and the occurrence of numerous mineral phases including a hydrous mineral (biotite) might suggest that the inclusion was initially trapped as a Mg-rich silicate–melt inclusion, and then various mineral phases in the composite inclusions were derived by complex reactions between the inclusion and host garnet during the high-grade metamorphism. The presence of quartzo-feldspathic rocks interlayered with garnetiferous rocks in the area supports the presence of a melt phase during the high-grade event.

Geothermobarometric calculations on the inclusion minerals gave a fairly wide ranges of pressures (8–10 kbar) and temperatures (780–1050 °C) which we interpret as the combined signature of both peak and retrograde metamorphism. Among these, the estimation using solubility of Al in orthopyroxene is regarded

as the indicator for the UHT conditions attained by these rocks. The result ($T>1050$ °C at 10 kbar) is consistent with the occurrence of sapphirine+quartz assemblage, which was first reported by Tateishi et al. (2004) from this locality and confirmed in this study. The Spr-1+quartz and Spr-2+quartz associations in the multiphase inclusion first identified in this study probably formed at the same *P–T* condition, although crystal size and shape of sapphirine as well as associations with other ferromagnesian minerals are apparently different from those of Tateishi et al.'s (2004) report. The other lower *P–T* results are considered to be the result of significant effect of retrograde metamorphism.

The unique inclusion assemblages in the Rajapalaiyam rock allow us to construct the *P–T* history of the rock. The close association of Spr-1 and Spl-1 around quartz (Fig. 3c) suggests that the Spl-1+quartz was an earlier stable assemblage and the Spr-1+quartz assemblage formed subsequently. From the observed textural relations, the *P–T* trajectory of this rock can be drawn in the FMAS petrogenetic grid (Fig. 7), taking into account the stability fields of spinel+quartz and sapphirine+quartz. Two possible *P–T* trajectories can explain the observed texture. One is a near-isobaric cooing from the stability field of spinel+quartz ($T>1200$ °C) towards the stability of sapphirine+quartz ($T\sim1050$ °C). Such an isobaric cooling path is consistent with the previously published *P–T* paths for the Madurai Block (e.g. Raith et al., 1997). However, such extreme thermal conditions of $T>1200$ °C peak metamorphic conditions have not been reported from UHT terranes in the world and could therefore be unrealistic. An alternate possibility is a pressure increase of about 2 kbar at 1050–1100 °C. The compression path would correspond to a counterclockwise trajectory, which has not so far been proposed from southern India. Interestingly, the following FMAS discontinuous reaction would take place as pressure increases (Fig. 7):

$$\mathrm{Grt} + \mathrm{Crd} \rightarrow \mathrm{Spr} + \mathrm{Opx} + \mathrm{Qtz} \quad (3)$$

The progress of this reaction could have generated the sapphirine+orthopyroxene+quartz assemblage in

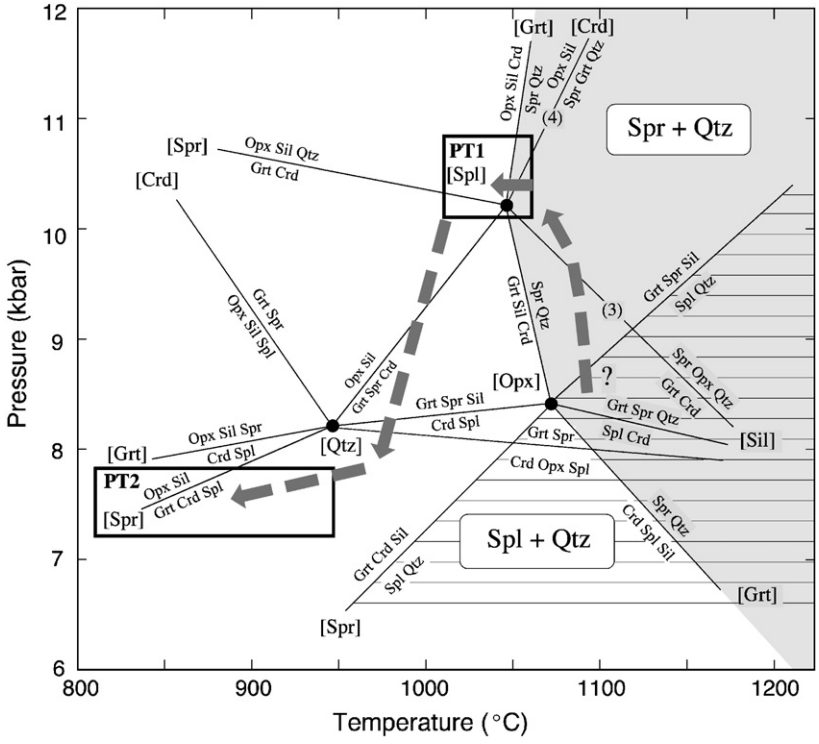

Fig. 7. Petrogenetic grid in the FMAS system (modified after Hensen and Harley, 1990; Harley, 1998; Motoyoshi, 1998). The stability fields of sapphirine+quartz and spinel+quartz are also shown. Here, we have chosen low fO_2 grid because magnetite is rare in this rock. Arrows indicate the approximate *P–T* trajectories inferred from the composite multiphase inclusion reported in this study. Reactions (3) and (4) are discussed in the text. Boxes PT1 and PT2 indicate *P–T* conditions calculated from Al-rich orthopyroxene and garnet–orthopyroxene–plagioclase–quartz assemblage, respectively. See text for further discussion.

the multiphase inclusion. Wavy boundary of host garnet with the inclusion (Figs. 2d, e and 3b), suggesting possibility of garnet being a reactant, further confirms that reaction (3) took place. Although we could not identify cordierite in the inclusion, it occurs as coarse-grained minerals together with quartz (Fig. 2a). We therefore regard that cordierite was a major constituent of the Mg-rich silicate-melt inclusion discussed above. The melt was probably trapped in garnet during prograde stage and then underwent UHT metamorphism to form the composite inclusion. Since other possible prograde assemblages have been completely modified by $T>1050$ °C UHT metamorphism, it is difficult to further consider the characteristics of such a prograde path.

A *P–T* path characterized by cooling should be located above the spinel invariant point because of the presence of sillimanite+orthopyroxene corona after garnet+sapphirine+quartz in an another pelitic granulite sample from Rajapalaiyam (Tsunogae and Santosh, in prep.), suggesting the following reaction:

$$\mathrm{Spr} + \mathrm{Qtz} + \mathrm{Grt} \rightarrow \mathrm{Opx} + \mathrm{Sil} \quad (4)$$

The high-pressure cooling is also supported by the orthopyroxene chemistry showing the *P–T* conditions of $T>1050$ °C and $P>10$ kbar. The area subsequently underwent near-isothermal decompression and formed orthopyroxene+cordierite corona around garnet by reaction (1) (Fig. 2c). The rock then cooled down to 7–8 kbar and 800–850 °C, as recorded in garnet–orthopyroxene–plagioclase–quartz assemblages.

In summary, detailed petrographic and mineralogical study on a composite, and an apparently "dirty", multiphase inclusion within garnet from a pelitic granulite has yielded valuable information on extreme crustal metamorphism at UHT conditions in the continental deep crust. The inclusion assemblage has yielded important clues on the nature of the *P–T* path. This study is the first of its kind reporting such complex and composite mineral inclusions in a UHT rock and demonstrates the use of inclusion petrography in understanding high-grade metamorphic processes. Available geochronological data based on U–Pb dating of monazite and zircon from UHT granulites in the Madurai Block (Santosh et al., unpublished) correlate the high grade metamorphism with a late Neoproterozoic–Cambrian thermal event coinciding with the collisional tectonics and subsequent extensional collapse associated with the final assembly of the Gondwana supercontinent. Our ongoing studies in this locality and other UHT granulite occurrences in the Madurai Granulite Block are expected to further unravel the tectonic history of this region.

Acknowledgements

Late Prof. A.S. Janardhan for introduced us to the Rajapalaiyam locality and we pay our homage to him, and dedicate this contribution to his memory. We also thank the staff at Gondwana Research Office in Trivandrum and Ms. Preetha Warrier for their helpful support. Special thanks are due to Dr. N. Nishida for his assistance on microprobe analyses. Tsunogae thanks Geology Department of the University of Johannesburg, and Santosh thanks Kochi University, Japan for facilities and support. This is a contribution to the Grant-in-Aid from the Japanese Ministry of Education, Sports, Culture, Science and Technology to Tsunogae (No. 17340158) and Santosh (No. 17403013). Professors K. Das and Y. Motoyoshi provided helpful comments that aided in improving our presentation. We thank these referees as well as Dr. K. Sajeev for his editorial comments.

References

Aranovich, L.Y., Berman, R.G., 1997. A new garnet–orthopyroxene thermometer based on reversed Al_2O_3 solubility in FeO–Al_2O_3–SiO_2 orthopyroxene. Am. Mineral. 82, 345–353.

Bertrand, P., Ellis, D.J., Green, D.H., 1991. The stability of sapphirine–quartz and hypersthene–sillimanite–quartz assemblages: an experimental investigation in the system FeO–MgO–Al_2O_3–SiO_2 under H_2O and CO_2 conditions. Contrib. Mineral. Petrol. 108, 55–71.

Carrington, D.P., Harley, S.L., 1995. Partial melting and phase relations in high-grade metapelites: an experimental petrogenetic grid in the KFMASH system. Contrib. Mineral. Petrol. 120, 270–291.

Dallwitz, W.B., 1968. Co-existing sapphirine and quartz in granulite from Enderby Land, Antarctica. Nature 219, 476–477.

Das, K., Dasgupta, S., Miura, H., 2003. An experimentally constrained petrogenetic grid in the silica-saturated portion of the system KFMASH at high temperatures and pressures. J. Petrol. 44, 1055–1075.

Das, K., Bose, S., Ohnishi, I., Dasgupta, S., 2006. Garnet–spinel intergrowths in ultrahigh-temperature granulite, Eastern Ghats, India: possible evidence of an early tschermak-rich orthopyroxene during prograde metamorphism. Am. Mineral. 91, 375–384.

Ellis, D.J., Sheraton, J.W., England, R.N., Dallwitz, W.B., 1980. Osumilite–sapphirine–quartz granulites from Enderby Land, Antarctica: mineral assemblages and reactions. Contrib. Mineral. Petrol. 72, 123–143.

Friedman, G.M., 1953. The spinel–silica reaction succession: a study of incompatible mineral phases. J. Geol. 62, 366–374.

Grew, E.S., 1980. Sapphirine+quartz association from Archean rocks in Enderby Land, Antarctica. Am. Mineral. 65, 821–836.

Grew, E.S., 1982. Osumilite in the sapphirine–quartz terrane of Enderby Land, Antarctica: implications for osumilite petrogenesis in the granulite facies. Am. Mineral. 67, 762–787.

GSI (Geological Survey of India), 1995. Geological and Mineral Map of Tamil Nadu and Pondicherry.

Harley, S.L., 1987. A pyroxene-bearing meta-ironstone and other pyroxene-granulites from Tonagh Island, Enderby Land, Antarctica: further evidence for very high temperature (>980 °C) Archaean regional metamorphism in the Napier Complex. J. Metamorph. Geol. 5, 341–356.

Harley, S.L., 1998. On the occurrence and characterization of ultrahigh-temperature crustal metamorphism. Spec. Publ.-Geol. Soc. Lond. 138, 81–107.

Harley, S.L., 2004. Extending our understanding of ultrahigh-temperature crustal metamorphism. J. Mineral. Petrol. Sci. 99, 140–158.

Harley, S.L., Green, D.H., 1982. Garnet–orthopyroxene barometry for granulites and peridotites. Nature 300, 697–701.

Hensen, B.J., Green, D.H., 1973. Experimental study of the stability of cordierite and garnet in pelitic compositions at high pressures and temperatures: III. Synthesis of experimental data and geological applications. Contrib. Mineral. Petrol. 38, 151–166.

Hensen, B.J., Harley, S.L., 1990. Graphical analysis of P-T-X relations in granulite facies metapelites. In: Ashworth, J.R., Brown, M. (Eds.), High-Temperature Metamorphism and Crustal Anatexis. Kluwer Academic Publishers, pp. 19–56.

Higgins, J.B., Ribbe, P.H., Herd, R.K., 1979. Sapphirine I: crystal chemical contributions. Contrib. Mineral. Petrol. 68, 349–356.

Kawasaki, T., Sato, K., 2002. Experimental study of Fe–Mg exchange reaction between orthopyroxene and sapphirine and its calibration as a geothermometer. Gondwana Res. 5, 741–747.

Kelsey, D.E., White, R.W., Holland, T.J.B., Powell, R., 2004. Calculated phase equilibria in K_2O–FeO–MgO–Al_2O_3–SiO_2–H_2O for sapphirine–quartz-bearing mineral assemblages. J. Metamorph. Geol. 22, 559–578.

Kretz, R., 1983. Symbols for rock-forming minerals. Am. Mineral. 68, 277–279.

Lal, R.K., 2003. Metamorphic evolution of granulites from Southern Indian Shield. Mem.-Geol. Soc. India 52, 61–108.

Lee, H.Y., Ganguly, J., 1988. Equilibrium compositions of coexisting garnet and orthopyroxene: experimental determinations in the system FeO–MgO–Al_2O_3–SiO_2, and applications. J. Petrol. 29, 93–113.

Motoyoshi, Y., 1998. Ultra-high temperature metamorphism of the Napier Complex, East Antarctica: a metamorphic perspective. J. Geol. Soc. Jpn. 104, 794–807 (in Japanese with English abstr).

Motoyoshi, Y., Hensen, B.J., 2001. F-rich phlogopite stability in ultra-high-temperature metapelites from the Napier Complex, East Antarctica. Am. Mineral. 86, 1404–1413.

Ouzegane, K., Boumaza, S., 1996. An example of ultrahigh-temperature metamorphism: orthopyroxene–sillimanite–garnet, sapphirine–quartz and spinel–quartz parageneses in Al–Mg granulites from In Hihaou, In Ouzzal, Hoggar. J. Metamorph. Geol. 14, 693–708.

Owen, V.J., Greenough, J.D., 1991. An empirical sapphirine–spinel Mg–Fe exchange thermometer and its application to high-grade xenoliths in the Popes Harbour dyke, Nora Scotia, Canada. Lithos 26, 317–332.

Perkins, D., Chipera, S.J., 1985. Garnet–orthopyroxene–plagioclase–quartz barometry: refinement and application to the English River subprovince and the Minnesota River valley. Contrib. Mineral. Petrol. 89, 69–80.

Perkins, D., Newton, R.C., 1981. Charnockite geobarometers based on coexistence garnet–pyroxene–plagioclase–quartz. Nature 292, 144–146.

Raith, M., Karmakar, S., Brown, M., 1997. Ultra-high-temperature metamorphism and multistage decompressional evolution of sapphirine granulites from the Palni hill ranges, Southern India. J. Metamorph. Geol. 15, 379–399.

Sajeev, K., Osanai, Y., 2004. Ultrahigh-temperature Metamorphism (1150 °C, 12 kbar) and multistage evolution of Mg-, Al-rich granulites from the Central Highland Complex, Sri Lanka. J. Petrol. 45, 1821–1844.

Sandiford, M., Powell, R., 1986. Pyroxene exsolution in granulites from Fyfe Hills, Enderby Land, Antarctica: evidence for 1000 °C metamorphic temperatures in Archean continental crust. Am. Mineral. 71, 946–954.

Santosh, M., Yokoyama, K., Biju-Sekhar, S., Rogers, J.J.W., 2003. Multiple tectonothermal events in the granulite blocks of southern India revealed from EPMA dating: implications on the history of supercontinents. Gondwana Res. 6, 29–63.

Sriramguru, K., Janardhan, A.S., Basava, S., Basavalingu, B., 2002. Prismatine and sapphirine bearing assemblages from Rajapalaiyam area, Tamil Nadu: origin and metamorphic history. J. Geol. Soc. India 59, 103–112.

Tateishi, K., Tsunogae, T., Santosh, M., Janardhan, A.S., 2004. First report of sapphirine+quartz assemblage from southern India: implications for ultrahigh-temperature metamorphism. Gondwana Res. 7, 899–912.

Tsunogae, T., Santosh, M., Osanai, Y., Owada, M., Toyoshima, T., Hokada, T., 2002. Very high-density carbonic fluid inclusions in sapphirine-bearing granulites from Tonagh Island in the Archean Napier Complex, East Antarctica: implications for CO_2 infiltration during ultrahigh-temperature (T>1100 °C) metamorphism. Contrib. Mineral. Petrol. 143, 279–299.

Tsunogae, T., Osanai, Y., Owada, M., Toyoshima, T., Hokada, T., Crowe, W.A., 2003. High fluorine pargasites in ultrahigh temperature granulites from Tonagh Island in the Archean Napier Complex, East Antarctica. Lithos 70, 21–38.